



The Second Scientific
Conference of Pure
and Applied Sciences

Special Volume , Number 1, pp.1 - 22, , August 2010

"Laminar Flow Forced Convection in Rectangular Cross-Sectional Duct"

Dr. Ala'a A. Mahdi
College of Eng./Mech. Dept.
Kufa University

Ammar F. Abdulwaheed
College of Eng./Mech. Dept.
Kufa University

Abstract

In this investigation, steady state two – dimensional laminar forced convection heat transfer of Newtonian and non-Newtonian fluids inside a duct of Rectangular shape has been studied numerically for a wide range of the Reynolds numbers of ($Re = 500$ and 10000) with the Power law index (n) of Power law model ranging from (0.1 to 2), and Prandtl number of ($Pr = 1$ and 10). Two types of boundary conditions have been considered. The first, when the side walls are heated with different uniform temperatures and the horizontal walls are insulated. The second, when the bottom wall is heated by applying a uniform heat flux while the other walls at the constant cold temperature. Also, the time independent non-Newtonian fluids under consideration were assumed obey to the Power law model. The numerical results of the values of average Nusselt number have been confirmed by comparing it to similar known previous works using the same boundary conditions. Good agreement was obtained. The results are presented in terms of isotherms and streamlines to show the behavior of the fluid flow and temperature. In addition, some graphs that represent the relation between average Nusselt number and the parameters mentioned previously are drawn. Also, the results show that the power law index (n) has, for a given Reynolds and Prandtl numbers, a large effect on the heat transfer rate at high Reynolds number. Twelve different correlations to show the dependence of the average Nusselt number on the power law index, the Reynolds and Prandtl numbers has been fund.

Keyword: Heat transfer forced convection, laminar flow

الخلاصة

في هذا البحث، تم إجراء دراسة عددية لانتقال الحرارة بالحمل القسري الطبقي المستقر ثنائي البعد لموائع نيوتنية وغير-نيوتنية في مجرى مستطيل الشكل ضمن مدى واسع لعدد رينولدز ($Re = 5 \times 10^2$ and 10^4) وللمقدار اللا بعدي للموديل الرياضي (Power law) يمتد من ($0.1 \leq n \leq 2$) ولعدد برانتل ضمن المدى ($Pr=1$ and 10). افترض نوعان من الظروف الحدية: الأول، عندما تكون الجدران الجانبية مسخنة إلى درجات حرارة مختلفة ومنظمة والجدران الأخرى معزولة. الثاني، عندما يكون الجدار السفلي مسخن بمصدر حراري ثابت بينما الجدران الأخرى عند درجة حرارة منخفضة وثابتة. كذلك افترض بأن سلوك الموائع غير- نيوتنية يخضع للموديل الرياضي (Power law). لقد تم مقارنة النتائج العددية لمعدل عدد نسلت لهذه الدراسة مع الدراسات السابقة باستعمال نفس الظروف الحدية، ووجد إن الحل العددي الحالي مقارب جدا لهذه البحوث. تم تمثيل نتائج الدراسة بدلالة خطوط درجات الحرارة الثابتة وخطوط الانسياب لبيان سلوك درجة الحرارة والجريان في المجرى. بالإضافة إلى رسومات بيانية أخرى تمثل علاقة معدل عدد نسلت مع المتغيرات المذكورة أعلاه. بالنسبة للحالتين التي تمت دراستها، فإن عملية انتقال الحرارة وطريقة تصرف الجريان تكون متأثرة بعدة عوامل كالمقدار اللا بعدي (n)، عدد رينولدز، وعدد برانتل. تم إيجاد اثنا عشر علاقة تقريبية تمثل اعتمادا دية معدل عدد نسلت على عدد رينولدز وعلى عدد برانتل والمقدار اللا بعدي (n).

Nomenclature

Symbol	Description	Unit
<i>Ar</i>	<i>Aspect ratio</i>	<i>Dimensionless</i>
<i>g</i>	<i>Gravitational acceleration</i>	<i>m/s²</i>
<i>H</i>	<i>Height of the duct</i>	<i>m</i>
<i>h</i>	<i>Heat transfer coefficient</i>	<i>W/m². K</i>
<i>K</i>	<i>Thermal conductivity</i>	<i>W/m. K</i>
<i>L</i>	<i>Width of the duct</i>	<i>m</i>
<i>m</i>	<i>Consistency coefficient</i>	<i>Kg/ sec⁽ⁿ⁾. m</i>
<i>n</i>	<i>The Power law index</i>	<i>Dimensionless</i>
<i>Nu</i>	<i>Nusselt number= $\frac{qL}{K(T_h - T_c)}$</i>	<i>Dimensionless</i>
<i>Nu_a</i>	<i>Average Nusselt number</i>	<i>Dimensionless</i>
<i>P</i>	<i>Pressure</i>	<i>Pa</i>
<i>Pr</i>	<i>Prandtl number = $\left(\frac{\nu}{\alpha}\right)$</i>	<i>Dimensionless</i>
<i>q</i>	<i>Heat flux</i>	<i>W/m²</i>
<i>Re</i>	<i>Reynolds number = $\left(\frac{\rho u_\infty L}{mn}\right)\left(\frac{u_\infty}{L}\right)^{(n-1)}$</i>	<i>Dimensionless</i>
<i>T</i>	<i>Temperature</i>	<i>K</i>
<i>u</i>	<i>Velocity in x-direction</i>	<i>m/s</i>
<i>v</i>	<i>Velocity in y-direction</i>	<i>m/s</i>
<i>x & y</i>	<i>Cartesian coordinate</i>	<i>m</i>

Greek Symbols	Description	Unit
<i>α</i>	<i>Thermal diffusivity</i>	<i>m²/s</i>
<i>f</i>	<i>Arbitrary function, f (x,y)</i>	
<i>ΔT</i>	<i>Temperature difference</i>	<i>K</i>
<i>Δx & Δy</i>	<i>Grid size in the x and y directions, respectively</i>	<i>m</i>

θ	Dimensionless temperature = $\begin{cases} \frac{T - T_c}{T_h - T_c} & \text{for B.C.1} \\ \frac{T - T_c}{\frac{qL}{k}} & \text{for B.C.2} \end{cases}$	
μ	<i>Dynamic viscosity</i>	<i>kg/m. s</i>
ν	<i>Kinematics viscosity</i>	<i>m²/s</i>
ρ	<i>Density</i>	<i>kg/m³</i>
τ_{xx}	$\begin{cases} \mu \frac{\partial u}{\partial y} & \text{For Newtonian Fluids} \\ m \left(\frac{\partial u}{\partial y} \right)^n & \text{For non- Newtonian Fluids} \end{cases}$	
τ_{yx}	<i>Normal stress in the y direction</i>	<i>N/m²</i>
ψ	<i>Stream function</i>	<i>m²/s</i>
ω	<i>Vorticity</i>	<i>1/s</i>

Subscripts

<i>c</i>	<i>Cold.</i>
<i>h</i>	<i>Hot.</i>
<i>i,j</i>	<i>Denotes nodal positions.</i>
<i>o</i>	<i>Reference condition.</i>

Superscript

*	<i>Dimensionless parameter</i>
---	--------------------------------

1. Introduction:

It is important to have knowledge of the characteristics of the forced convective heat transfer in steady laminar non-Newtonian flow through ducts with arbitrary shaped cross-sections in order to exercise proper control over the performance of the heat exchanger, and the heat transfer in the combined entry region of rectangular ducts is of particular interest in the design of compact heat exchangers. Forced convection heat transfer of Newtonian and non – Newtonian fluids through ducts has been the subject of several studies in the last years. The attention is due to the wide range of applications such as petrochemical industries, heat exchangers that are widely used would include boilers and condensers in steam power plant and petrochemical plants [1]. In these applications passages are generally short and usually composed of cross-section such as rectangular geometry. Also, food, polymer, petrochemical, rubber, paint and biological industries fluids with non-Newtonian behavior are encountered. Forced convection heat transfer through ducts involves different aspect of problems. This variety of problems comes from possibly geometry characteristic of ducts, kind of fluid, nature of fluid flow, etc. In the present work, a numerical study is performed to analyze the laminar forced convective heat transfer of Newtonian and non – Newtonian fluids through rectangular duct under two different cases of thermal boundary conditions. The fluid motion and heat transfer are affected by Reynolds number, Prandtl number, and power law index (n) of Power law model [2]. The power law index (n) determines the nature of fluid, that is, Newtonian ($n=1$) and non – Newtonian fluids ($1 > n < 1$).

2. Mathematical Formulation:

Consider steady state, two – dimensional, laminar incompressible flow of a non – Newtonian fluid with constant physical properties (kinematics viscosity and thermal diffusivity) flowing through a duct have rectangular cross sectional area of width (L) and height (h) under two different cases of thermal boundary conditions, these boundary conditions are:

Case(I) :-

The vertical walls are heated with different uniform temperatures (T_h & T_c) and the horizontal walls are perfectly insulated (B.C.1), as shown in (Fig.1a).

Case(II) :-

The lower wall is heated by applying a uniform heat flux (q) and the other walls are isothermally cooled (T_c) (B.C.2), as shown in (Fig.1b).

The governing equations are the following:

$$\frac{\partial u}{\partial x} + \frac{\partial v}{\partial y} = 0 \quad (1)$$

$$\rho_o (u \frac{\partial u}{\partial x} + v \frac{\partial u}{\partial y}) = -\frac{\partial p}{\partial x} + \frac{\partial \tau_{xx}}{\partial x} + \frac{\partial \tau_{yx}}{\partial y} \quad (2)$$

$$\rho_o (u \frac{\partial v}{\partial x} + v \frac{\partial v}{\partial y}) = -\frac{\partial p}{\partial y} + \frac{\partial \tau_{xy}}{\partial x} + \frac{\partial \tau_{yy}}{\partial y} \quad (3)$$

$$u \frac{\partial T}{\partial x} + v \frac{\partial T}{\partial y} = \alpha (\frac{\partial^2 T}{\partial x^2} + \frac{\partial^2 T}{\partial y^2}) \quad (4)$$

In the above equations, (u, v, α, P, T) are the fluid velocity components (Fig.1), the thermal diffusivity, the pressure and the temperature. In fact Eqs.(1) to (4) are system of partial differential equations. They are represent the base for forced convection phenomenon for 2D ducts, presented by mass, momentum and energy conservation equations.

As mentioned in Ref.[3], the Power law model for non – Newtonian fluids can be represented as:

$$\tau = m (\frac{\partial u}{\partial y})^n \quad (5)$$

Hence, the shear stresses:

$$\tau_{xx} = 2m (\frac{\partial u}{\partial x})^n \quad (6)$$

$$\tau_{yy} = 2m (\frac{\partial v}{\partial y})^n \quad (7)$$

$$\tau_{xy} = \tau_{yx} = m (\frac{\partial u}{\partial y} + \frac{\partial v}{\partial x})^n \quad (8)$$

where m is Consistency coefficient for the power law model.

Since it proves to be more convenient to work in terms of a stream function and vorticity, the stream function $\psi(x,y)$ is introduced in the usual manner:

$$u = \frac{\partial \psi}{\partial y} \quad \& \quad v = -\frac{\partial \psi}{\partial x} \quad (9)$$

It is evident from Eq.(9) that the stream function satisfies the continuity equation identically.

Further more, for this plane flow field, the only non – zero component of the vorticity is:

$$\omega = \frac{\partial v}{\partial x} - \frac{\partial u}{\partial y} \quad (10)$$

Combining the definition of vorticity and the velocity components in terms of the stream function, and cross – differentiating the Eqs.(2) and (3) to reduce the number of equations and

eliminate the pressure terms, and substituting for (τ) from Eqs.(6 - 8), a new set of equations is obtained with independent variables ψ , ω and T :

$$\frac{\partial^2 \psi}{\partial x^2} + \frac{\partial^2 \psi}{\partial y^2} = -\omega \tag{11}$$

$$\rho \left[\frac{\partial \psi}{\partial y} \frac{\partial \omega}{\partial x} - \frac{\partial \psi}{\partial x} \frac{\partial \omega}{\partial y} \right] = \left[\frac{\partial^2 \omega}{\partial x^2} + \frac{\partial^2 \omega}{\partial y^2} \right] + mn \left[\frac{\partial S_1}{\partial x} - \frac{\partial S_2}{\partial y} + 2 \frac{\partial}{\partial x} (S_3 - S_4) \right] + S_I \tag{12}$$

$$\frac{\partial \psi}{\partial y} \frac{\partial T}{\partial x} - \frac{\partial \psi}{\partial x} \frac{\partial T}{\partial y} = \alpha \left(\frac{\partial^2 T}{\partial x^2} + \frac{\partial^2 T}{\partial y^2} \right) \tag{13}$$

where;

$$S_I = \left(\frac{\partial^4 \psi}{\partial x^4} + \frac{\partial^4 \psi}{\partial y^4} + 2 \frac{\partial^4 \psi}{\partial x^2 \partial y^2} \right) \tag{14}$$

$$S_1 = \left(\frac{\partial^2 \psi}{\partial y^2} - \frac{\partial^2 \psi}{\partial x^2} \right)^{n-1} \left(\frac{\partial^3 \psi}{\partial x \partial y^2} - \frac{\partial^3 \psi}{\partial x^3} \right), \quad S_2 = \left(\frac{\partial^2 \psi}{\partial y^2} - \frac{\partial^2 \psi}{\partial x^2} \right)^{n-1} \left(\frac{\partial^3 \psi}{\partial y^3} - \frac{\partial^3 \psi}{\partial y \partial x^2} \right) \tag{15}$$

$$S_3 = - \left(- \frac{\partial^2 \psi}{\partial y \partial x} \right)^{n-1} \left(\frac{\partial^3 \psi}{\partial x \partial y^2} \right), \quad \& \quad S_4 = \left(\frac{\partial^2 \psi}{\partial y \partial x} \right)^{n-1} \left(\frac{\partial^3 \psi}{\partial x \partial y^2} \right) \tag{16}$$

Now, the mathematical problem formulated above is placed in dimensionless form by defining the new dimensionless variables [4]:

$$x^* = \frac{x}{L}, \quad y^* = \frac{y}{h}$$

$$\theta = \begin{cases} \frac{T - T_c}{T_h - T_c} & \text{for B.C.1} \\ \frac{T - T_c}{\frac{qL}{k}} & \text{for B.C.2} \end{cases}$$

$$\psi^* = \frac{\psi}{u_\infty L}, \quad \omega^* = \frac{\omega L}{u_\infty}$$

Inserting all the dimensionless variables into Eqs.(11) to (16), yield the following final non – dimensional equations:

$$\frac{\partial^2 \psi^*}{\partial x^{*2}} + \frac{\partial^2 \psi^*}{\partial y^{*2}} = -\omega^* \tag{17}$$

$$\left[\frac{\partial \psi^*}{\partial y^*} \frac{\partial \omega^*}{\partial x^*} - \frac{\partial \psi^*}{\partial x^*} \frac{\partial \omega^*}{\partial y^*} \right] = \left(\frac{1}{\text{Re}} \left[\frac{\partial^2 \omega^*}{\partial x^{*2}} + \frac{\partial^2 \omega^*}{\partial y^{*2}} \right] \right) + \left(\frac{1}{\text{Re}} \left[\frac{\partial S_1^*}{\partial x^*} - \frac{\partial S_2^*}{\partial y^*} + 2 \frac{\partial}{\partial x^*} (S_3^* - S_4^*) \right] \right) + \left(\frac{1}{\text{Re}} \right) S_I^* \tag{18}$$

$$\frac{\partial \psi^*}{\partial y^*} \frac{\partial \theta}{\partial x^*} - \frac{\partial \psi^*}{\partial x^*} \frac{\partial \theta}{\partial y^*} = \text{Pr} \left(\frac{\partial^2 \theta}{\partial x^{*2}} + \frac{\partial^2 \theta}{\partial y^{*2}} \right) \quad (19)$$

where;

$$S_I^* = \left(\frac{\partial^4 \psi^*}{\partial x^{*4}} + \frac{\partial^4 \psi^*}{\partial y^{*4}} + 2 \frac{\partial^4 \psi^*}{\partial x^{*2} \partial y^{*2}} \right) \quad (20)$$

$$S_1^* = \left(\frac{\partial^2 \psi^*}{\partial y^{*2}} - \frac{\partial^2 \psi^*}{\partial x^{*2}} \right)^{n-1} \left(\frac{\partial^3 \psi^*}{\partial x^* \partial y^{*2}} - \frac{\partial^3 \psi^*}{\partial x^{*3}} \right) \quad (21)$$

$$S_2^* = \left(\frac{\partial^2 \psi^*}{\partial y^{*2}} - \frac{\partial^2 \psi^*}{\partial x^{*2}} \right)^{n-1} \left(\frac{\partial^3 \psi^*}{\partial y^{*3}} - \frac{\partial^3 \psi^*}{\partial y^* \partial x^{*2}} \right) \quad (22)$$

$$S_3^* = - \left(- \frac{\partial^2 \psi^*}{\partial y^* \partial x^*} \right)^{n-1} \left(\frac{\partial^3 \psi^*}{\partial x^* \partial y^{*2}} \right) \quad \& \quad S_4^* = \left(\frac{\partial^2 \psi^*}{\partial y^* \partial x^*} \right)^{n-1} \left(\frac{\partial^3 \psi^*}{\partial x^* \partial y^{*2}} \right) \quad (23)$$

$\text{Pr} = \frac{\nu}{\alpha}$ is the Prandtl number.

$\text{Re} = \left(\frac{\rho u_\infty L}{mn} \right) \left(\frac{u_\infty}{L} \right)^{n-1}$ is the Reynolds number.

3. Numerical Method :

Numerical methods have been developed to handle problems involving nonlinearities in the describing equations, or complex geometries involving complicated boundary conditions. A finite-difference technique is applied to solve the governing equations. These three equations (Eqs.(17), (18), and (19)) are to be solved in a given region subject to the condition that the values of the stream function, temperature, and the vorticity, or their derivatives, are prescribed on the boundary of the domain. The finite difference approximation of the governing equations is based on dividing the interval ($1 \geq x^* \geq 0$) into (m) equal segments separated by ($m+1$) nodes. Likewise, the (y^*) interval was divided into (n) segments. The usual procedure for obtaining the form of partial differential equation with finite-difference method [5 & 6] is to approximate all the partial derivatives in the equation by means of their Taylor series expansions.

Eq.(17) can be approximated using central – difference at the representative interior point (i,j), thus, Eq.(17) can be written for regular mesh as:

$$\psi_{i,j}^* = [(\psi_{i+1,j}^* + \psi_{i-1,j}^*)(\Delta y^2) + (\psi_{i,j+1}^* + \psi_{i,j-1}^*)(\Delta x^2) + (\Delta x^2)(\Delta y^2)\omega_{i,j}^*] / [(2\Delta y^2 + (2\Delta x^2))] \quad (24)$$

Also, a central – difference formulation can be used for Eqs.(18), and (19). But this problem will need to be solved for reasonably high values of Reynolds numbers; it is known that such a formulation may not be satisfactory owing to the loss of diagonal dominance in the sets of difference equations, with resulting difficulties in convergence when using an iterative procedure.

A forward – backward technique can be introduced to maintain the diagonal dominance coefficient of $(\omega_{i,j})$ in Eq.(18) and $(\theta_{i,j})$ in Eq.(19) which determines the main diagonal elements of the resulting linear system; this technique is outlined as follows [7]:

$$\text{Set; } \gamma = \psi_{i+1,j}^* - \psi_{i-1,j}^* \quad \text{and} \quad \beta = \psi_{i,j+1}^* - \psi_{i,j-1}^* \quad (25)$$

Then approximate Eq.(18) by:

$$\frac{1}{\text{Re}} \left[\frac{(\omega(i+1, j) - 2\omega(i, j) + \omega(i-1, j))}{\Delta x^2} + \frac{(\omega(i, j+1) - 2\omega(i, j) + \omega(i, j-1))}{\Delta y^2} \right] + \frac{1}{\text{Re}} \left[\left(\frac{\partial S_1^*}{\partial x^*} - \frac{\partial S_2^*}{\partial y^*} + 2 \frac{\partial}{\partial x^*} (S_3^* - S_4^*) \right) + S_l^* \right] + \left(\frac{\gamma}{\Delta x^2} \frac{\partial \omega^*}{\partial y^*} - \frac{\beta}{\Delta y^2} \frac{\partial \omega^*}{\partial x^*} \right) = 0 \quad (26)$$

and Eq.(19) by:

$$\text{Pr} \left(\frac{\theta_{i+1,j} - 2\theta_{i,j} + \theta_{i-1,j}}{\Delta x^2} \right) + \left(\frac{\theta_{i,j+1} - 2\theta_{i,j} + \theta_{i,j-1}}{\Delta y^2} \right) + \left[\frac{\gamma}{\Delta x^2} \frac{\partial \theta}{\partial y^*} - \frac{\beta}{\Delta y^2} \frac{\partial \theta}{\partial x^*} \right] = 0 \quad (27)$$

Now, if

$$\gamma \geq 0, \quad \frac{\partial f}{\partial y} = \frac{f_{i,j+1} - f_{i,j}}{\Delta y}, \quad (b_1 = 1), \quad \text{and} \quad (b_2 = 0)$$

$$\gamma < 0, \quad \frac{\partial f}{\partial y} = \frac{f_{i,j} - f_{i,j-1}}{\Delta y_r}, \quad (b_1 = 0), \quad \text{and} \quad (b_2 = 1)$$

if $\beta \geq 0, \quad \frac{\partial f}{\partial x} = \frac{f_{i,j} - f_{i-1,j}}{\Delta x_r}, \quad (a_1 = 1), \quad \text{and} \quad (a_2 = 0)$

$$\beta < 0, \quad \frac{\partial f}{\partial x} = \frac{f_{i+1,j} - f_{i,j}}{\Delta x}, \quad (a_1 = 0), \quad \text{and} \quad (a_2 = 1)$$

To assure the diagonal dominance of the coefficient matrix for $(\omega_{i,j}^*)$ and $(\theta_{i,j})$, which depends on the sign of (γ) and (β) , Eqs.(18) and (19) are expressed in the following difference forms:

$$\begin{aligned}
 \omega_{i,j}^* = & [(0.5\gamma b_1(\Delta x)(\Delta y) + \frac{I}{Re}(\Delta x^2))\omega_{i,j+1}^* + (0.5\beta a_1(\Delta x)(\Delta y) + \frac{I}{Re}(\Delta y^2))\omega_{i-1,j}^* \\
 & - (0.5\beta a_2(\Delta x)(\Delta y) - \frac{I}{Re}(\Delta y^2))\omega_{i+1,j}^* - (0.5\gamma b_2(\Delta x)(\Delta y) - \frac{I}{Re}(\Delta x^2))\omega_{i,j-1}^* + \\
 & \frac{I}{Re}(\Delta x^2)(\Delta y^2)(\frac{S_{1i+a_2,j}^* - S_{1i-a_1,j}^*}{(\Delta x)} - \frac{S_{2i,j+b_1}^* - S_{2i,j-b_2}^*}{(\Delta y)} + 2\frac{S_{3i+a_2,j}^* - S_{4i+a_2,j}^* - (S_{3i-a_1,j}^* - S_{4i-a_1,j}^*)}{(\Delta x)}) \\
 & + \frac{1}{Re} S_{1i,j}^* (\Delta x^2)(\Delta y^2)]/[2(\Delta y^2) + 2(\Delta x^2) + (\Delta x^2)(\Delta y^2)(\frac{\gamma}{2(\Delta x)(\Delta y)^{b_1}(-\Delta y)^{b_2}} \\
 & + \frac{\beta}{2(\Delta y)(\Delta x)^{a_1}(-\Delta x)^{a_2}})]
 \end{aligned} \tag{28}$$

$$\begin{aligned}
 \theta_{i,j} = & [\text{Pr} (0.5\gamma b_1(\Delta x)(\Delta y) + (\Delta x^2))\theta_{i,j+1} + (0.5\beta a_1(\Delta x)(\Delta y) + (\Delta y^2))\theta_{i-1,j} \\
 & - (0.5\beta a_2(\Delta x)(\Delta y) - (\Delta y^2))\theta_{i+1,j} - (0.5\gamma b_2(\Delta x)(\Delta y) - (\Delta x^2))\theta_{i,j-1}] / \\
 & [2(\Delta y^2) + 2(\Delta x^2) + (\Delta x^2)(\Delta y^2)(\frac{\gamma}{2(\Delta x)(\Delta y)^{b_1}(-\Delta y)^{b_2}} + \frac{\beta}{2(\Delta y)(\Delta x)^{a_1}(-\Delta x)^{a_2}})]
 \end{aligned} \tag{29}$$

An under – relaxation technique can be applied to accelerate the convergence of Eq.(28); the expression is used in this technique presented in the following :

$$\omega_{i,j}^{*k+1} = (1 - Fv)\omega_{i,j}^{*k} + (Fv)\omega_{i,j}^* \text{ (computed)}$$

Where (Fv) is the relaxation factor for the vorticity. The value of this relaxation factor is in the range of (0 to 2).

In order to obtain results of the conservation equations, The above equations (Eqs.(24), (28), and (29)) are subjected to the following boundary conditions [8]:

Case (I) :-

$$\begin{aligned}
 0 \leq x^* \leq 1 \quad y^* = 0 \quad \psi^* = \frac{\partial \psi^*}{\partial y^*} = 0 \quad \frac{\partial \theta}{\partial y^*} = 0 \\
 0 \leq x^* \leq 1 \quad y^* = Ar \quad \psi^* = \frac{\partial \psi^*}{\partial y^*} = 0 \quad \frac{\partial \theta}{\partial y^*} = 0 \\
 x^* = 0 \quad 0 \leq y^* \leq Ar \quad \psi^* = \frac{\partial \psi^*}{\partial x^*} = 0 \quad \theta = \theta_h \\
 x^* = 1 \quad 0 \leq y^* \leq Ar \quad \psi^* = \frac{\partial \psi^*}{\partial x^*} = 0 \quad \theta = \theta_c
 \end{aligned}$$

Case (II) :-

$$\begin{aligned}
 0 \leq x^* \leq 1 \quad y^* = 0 \quad \psi^* = \frac{\partial \psi^*}{\partial y^*} = 0 \quad \frac{\partial \theta}{\partial y^*} + 1 = 0 \\
 0 \leq x^* \leq 1 \quad y^* = Ar \quad \psi^* = \frac{\partial \psi^*}{\partial y^*} = 0 \quad \theta = \theta_c \\
 x^* = 0 \quad 0 \leq y^* \leq Ar \quad \psi^* = \frac{\partial \psi^*}{\partial x^*} = 0 \quad \theta = \theta_c \\
 x^* = 1 \quad 0 \leq y^* \leq Ar \quad \psi^* = \frac{\partial \psi^*}{\partial x^*} = 0 \quad \theta = \theta_c
 \end{aligned}$$

Also, the following finite difference equation for the vorticity at a wall is adopted as the boundary condition for the vorticity equation:

$$\omega_o = \frac{3(\psi_o - \psi_1)}{\Delta n^2} - \frac{\omega_1}{2} \quad \text{where, } \Delta n = \Delta y \text{ or } \Delta x$$

The physical quantities of interest in this problem are the local Nusselt number along the heated wall [9], defined by:

$$Nu = \frac{qL}{k(T_h - T_c)} \tag{30}$$

and also the average Nusselt number, which is defined as:

Case (I) :-

$$Nu_a = \int_0^1 \left. \frac{\partial \theta}{\partial x^*} \right|_{x^*=0 \text{ or } 1} dy \tag{31}$$

Case (II) :-

$$Nu_a = \int_0^1 \frac{1}{\theta_h} dx \tag{32}$$

The numerical work starts with giving the distributions of stream function and temperature for forced convection as the zeroth-order approximation. Then, obtain the zeroth-order approximation of vorticity: Based on these old fields, equation (28) is used to determine point-by-point the new (ψ^*) field, and equation (29) is used to determine the new (ω^*), while the energy equation (29) is used to determine the new (θ) field. The iteration process is terminated under the following condition:

$$\sum_{i,j} |\tau^{r+1}_{i,j} - \tau^r_{i,j}| / \sum_{i,j} \tau^{r+1}_{i,j} \leq 10^{-5} \tag{33}$$

(r) denotes the iteration step. (ψ^* , ω^* , or θ); where, (τ) stands for either

Before starting the computational solution, the grid independence of the results must be tested. Thus, numerical experiments have been carried out to solve a two – dimensional problem in which the Power law index ($n = 1$). The Prandtl number in this test is set to be (6.7), while the grid size varies from (10×10) to (60×60) for different values of Reynolds number as shown in Fig.(2). It is found that the change in the Nusselt number for grid size of (35×35) and (45×45) is less than (0.8) percent for the range of Reynolds number ($10^3 \leq Re \leq 10^5$). Therefore, the number of grid that is adopted in the present study is (35×35) for both two cases. The number of grid point was selected as a compromise between accuracy and speed of computation.

4. Results and discussion :

Case (I) :- under B.C.1

a-Temperature and Flow Fields:

The contour lines of the temperature distribution and flow fields for different values of system parameters are presented in Figs.(3) to (11). In this case, the energy is transported from hot wall to cold wall by conduction ($25 \leq Nu_a \leq 38$) at Reynolds number and Power law index (n) are less than (10) and (1) respectively. In the conduction regime, the isotherms are almost parallel to isothermal walls. The small value of (ψ)_{max} characterizes a very weak convective flow. However, an increase in Re or (n) results in an asymmetric flow pattern producing streamlines near the walls, and change the direction of the isotherms, as shown in Figs.(3) and (4). As Re is increased further for a given n or n is increased for high values of Re , the streamlines more closer to the vertical walls, producing strong boundary layer effects on the isothermal walls. As a result, the stratified region become bigger, as shown in Figs.(5) and (6). Although the flow remains unicellular at all Reynolds numbers and Power law index (n), the velocity in the upper right corner and lower left corner increases substantially. Fig.(7) represent the variation of stream function with Reynolds number compared for different values of Power law index and ($Pr=10$, $Ar=1.0$). At low Reynolds ($Re < 2000$), ψ seems to be invariable with Pr , Ar , and n (i.e. at $n < 0.2$), this is due to dominance of conduction as mentioned before. At higher Re , the stream function (ψ) increases with increasing Pr or n . It is also seen that the value of ψ_{max} increases and reaches the peak value at $Re = 10^4$, for $Pr = 100$, $Ar=1.5$, and $n = 2$. It is also show that the peak value of ψ_{max} depends on Re and n at a fixed Pr and Ar .

b -Effect of Aspect Ratio:

Effect of aspect Ratio on the flow pattern can be inferred with reference to Figs. (9) and (10). It is worth while to note that any increase in aspect ratio increase the appearance of convective mode. The reasoning for this is as follows. As the aspect ratio increase, the isothermal walls become bigger than the insulated walls. The results of the numerical computations for streamlines and isotherms at ($Re=10^4$) with ($Ar= 0.5, 1, \text{ and } 1.5$) are plotted in Figs. (9 & 10). As depicted in this Figures. This is expected because the distance between isothermal wall at ($Ar=1.0$) is bigger than of ($Ar=1.5$). Figs. (11) and (12) are represent the relation between Nusselt number (Nu_a) and aspect ratio (Ar) compared for different value of Reynolds number. At low aspect ratio (Ar), (Nu_a) seems to be invariable with Reynolds number this is due to dominance of condition as mentioned before. At higher aspect ratio (Ar) or when convective becomes dominant, (Ar) increasing Nusselt number (Nu_a), since for a higher aspect ratio, the path along which the ascending flow is heated is longer.

c-Heat Transfer Coefficient:

To understand the heat transfer process by forced convection, it must be to evaluate the heat transfer coefficient (h), but to make the present work having generality, the calculated results must be in dimensionless form. Therefore, it must be needed to evaluate Nusselt number (Nu) as a function of influence parameters. Fig.(8) shows the variation of average Nusselt number versus Reynolds number with different values of Power law index and Prandtl number ($Pr=10$) on the hot wall of the duct. It is seen that for range of Reynolds number before (2000), the rate of increase in Nu_a against Re for different values of n at a fixed Ar and Pr is relatively small. But, Nu_a increases rapidly as n increases for $Re \geq 10^4$ expressing the increase of convective heat transfer. It is also noticed that the effect of n on Nu_a is more pronounced as the Re numbers increase.

Case (II) :- under B.C.2

a-Temperature and Flow Fields:

Figs.(13) to (22) show the contour lines of the temperature distribution and flow fields for the present case. A change in boundary conditions from (Case (I)) to (Case (II)), modifies the temperature and velocity fields significantly. Fig.(15a) shows the streamlines at $Re = 10^4$, $n = 0.1$, $Ar=0.5$, and $Pr = 10$. This flow exhibits one rotating cell, covering all the region. This cell has a maximum magnitude ($\psi_{max} = 0.133$). This cell is symmetric about the center line of the region. The convective velocity near the wall is lower than that along the line of symmetry. As Re or n increases more the streamlines moves closer toward the line of symmetry, producing a strong boundary layer effects on the middle region of the duct, and increase the convective velocity in the

upper and lower middle region of the duct as shown in Figs.(13) and (15). Fig.(17) represent the variation of ψ with Re for different values of n at $Ar=1.0$ and $Pr=10$. Furthermore, the isotherms are symmetric about the vertical line at $x = 0.5$ for different values of system parameters, and the maximum temperature θ_{max} always occurs at the middle of the lower wall, and is a function of Re , n , Ar , and Pr . Furthermore any increase in Re or n caused a high change in temperature field which concentrated in the small region near the top surface as shown in Figs.(14), (16), and (20). The isotherms in the upper region are almost horizontal for a large portion of the duct which allows a large amount of heat to be rejected on the top wall, and gives the vertical walls weaker effects than that in case (I). For a fixed Re , the amount of energy removed on the top wall is increased with n . Indeed, the large scale modification in the temperature and flow fields due to the change in the boundary conditions from (Case(I)) to (Case (II)) is mostly concentrated in small region, near the top surface. A significant amount of energy is also rejected at the vertical surfaces when the Re or n is small. However, the heat transfer on this surfaces decreases with an increase in Re or n which clearly implies that the effect of the vertical walls boundary Conditions diminishes with higher velocities or higher Re .

b- Effect of Aspect Ratio:

Effect of aspect Ratio on the flow pattern in case (II) can be inferred with reference to Figs.(19) and (20). It is worth while to note that any decrease in aspect ratio due to increase the appearance of convective mode. The reasoning for this is as follows. As the aspect ratio increase, the heat flux walls become smaller. Thus, there area for convective contribution, compared to the path for flow, Also it is seen the flow at ($Re = 500$) for ($Ar=1$). Now, different values of aspect ratio will be taken examine the appearance of the flow. The results of the numerical computations for streamlines and isotherms at ($Re=10^4$) with ($Ar= 0.5, 1$ and 1.5) are plotted in Figs.(19) and (20) which show the value of aspect ratio. As depicted in this Figures. This is expected because the distance between heat flux wall at ($Ar=1$) is bigger than of ($Ar=1.5$). It is worthwhile to note that any increase in aspect ratio due to decrease the appearance of convective mode. Figs.(21) and (22) are represent the relation between Nusselt number (Nu_a) and aspect ratio (Ar) compared for different value of Reynolds number. At low aspect ratio (Ar), (Nu_a) seems to be invariable with Reynolds number this is due to dominance of condition as mentioned before. At higher aspect ratio (Ar) or when convective becomes dominant, (Ar) decreasing Nusselt number (Nu_a), since for a higher aspect ratio, the path along which the ascending flow is heated is smaller.

c-Heat Transfer Coefficient:

The average Nusselt number as defined by Eq.(33) is presented in Fig.(18). It is seen that for Re and n are less than (2000) and (0.2) respectively, the rate of increase in Nu_a is relatively small. Then, Nu_a increases rapidly as Re or n increases expressing the existence and increase of convective heat transfer. As already indicated by the temperature field, the average Nusselt number for the present case is higher than that for the case (I) for the same given condition.

Finally, twelve correlation equations have been predicted depending on variation of Reynolds number, Prandtl number, and Power law index of the Power law model for both two cases, by using least square method.

Case (I): under B.C.1

a) At ($Ar=0.5$):

$$Nu_a = 0.301986 Re^{0.461} Pr^{0.873} n^{0.386}, \quad 0.1 \leq n \leq 0.5, \quad R = 0.953 \quad (34)$$

and,

$$Nu_a = 0.085 Re^{0.567} Pr^{0.83} n^{0.4}, \quad 0.5 < n \leq 2, \quad R = 0.942 \quad (35)$$

b) At ($Ar=1$):

$$Nu_a = 16.68 Re^{0.556} Pr^{0.785} n^{2.2}, \quad 0.1 \leq n \leq 0.5, \quad R = 0.912 \quad (36)$$

and,

$$Nu_a = 0.037 Re^{0.656} Pr^{0.953} n^{1.5}, \quad 0.5 < n \leq 2, \quad R = 0.949 \quad (37)$$

c) At ($Ar=1.5$):

$$Nu_a = 0.264 Re^{0.932} Pr^{0.832} n^{1.47}, \quad 0.1 \leq n \leq 0.5, \quad R = 0.8991 \quad (38)$$

and,

$$Nu_a = 0.0216 Re^{0.832} Pr^{0.759} n^{0.987}, \quad 0.5 < n \leq 2, \quad R = 0.962 \quad (39)$$

Case (II): under B.C.2

a) At ($Ar=0.5$):

$$Nu_a = 76.335 Re^{0.367} Pr^{0.197} n^{1.036}, \quad 0.1 \leq n \leq 0.5, \quad R = 0.89 \quad (40)$$

and,

$$Nu_a = 7.233 Re^{0.149} Pr^{0.855} n^{0.78}, \quad 0.5 < n \leq 2, \quad R = 0.959 \quad (41)$$

b) At ($Ar=1$):

$$Nu_a = 75.33 Re^{0.989} Pr^{0.88} n^{1.036}, \quad 0.1 \leq n \leq 0.5, \quad R = 0.899 \quad (42)$$

and,

$$Nu_a = 6.77 Re^{0.149} Pr^{0.899} n^{0.069}, \quad 0.5 < n \leq 2, R = 0.959 \quad (43)$$

c) At ($Ar=1.5$):

$$Nu_a = 86.66 Re^{0.901} Pr^{0.878} n^{1.036}, \quad 0.1 \leq n \leq 0.5, R = 0.887 \quad (44)$$

and,

$$Nu_a = 9.677 Re^{0.149} Pr^{0.899} n^{0.699}, \quad 0.5 < n \leq 2, R = 0.959 \quad (45)$$

The above correlations are acceptable in the range of Reynolds number (500 to 10^4), Prandtl number (1 to 100), and Power law index ($n = 0.1$ to 2).

To ensure that these approximation correlations are usable, the coefficient of determination (R) had been obtained for each equation. The minimum value of (R) was (0.887), that means these approximate equations are good for predicting the value of average Nusselt number.

Now, the values of average Nusselt number have been compared with those of other investigators using the same boundary conditions to show the validation of the present numerical results.

To compare the present numerical results with those of convection heat transfer in duct for Newtonian fluids. The power law index (n) in Eq.(28) is set to one, and the comparison has been done with a Rectangular duct subjected to different temperature on it's vertical sides with the top and bottom are insulated. Table (1) show this comparison with the studies of Y., S., Muzychka.[6] .

A similar comparison has been made with the solution of convection heat transfer in rectangular duct filled with Newtonian fluids and subjected to an ascending constant heat flux, this is shown in Table(2). The comparisons have been done for different values of Reynolds numbers (10^3 to 10^6) and at Prandtl number of ($Pr = 0.71$, and 100). The results for ($Re = 10^4$ and 10^5) show a good agreement with those presented by Y., S., Muzychka [6] has analyzed a similar problem for different values of Reynolds numbers. The comparison with his results show agreements within ($\pm 4\%$). as shown in Table (1), there are some differences between the present work and this of Y., S., Muzychka [6]. These differences are due to the finite difference approximation and the computing system used.

9. Conclusions :-

The present numerical solutions for laminar forced convection heat transfer of Newtonian and non-Newtonian fluids for rectangular duct under two different cases of boundary conditions (B.C.1 and B.C.2), show that the effect of the geometry and the type of fluid on the flow development and the energy transfer are dominant and complex. The main conclusions of the present study are:

1- For the two cases that have been solved, it has been demonstrated that the average Nusselt number is a strong function of Reynolds number, Power law index (n), and Prandtl number, also the results show the average Nusselt number:

a- Increases as (Re) increases, for a given values of (n) and (Pr).

b- Increases as (n) increases except for ($n < 0.1$) at ($Re \leq 2000$), for a given value of (Pr).

c- Increases as (Pr) increases, for a given values of (Re) and (n).

d- Nu_a for the second case of boundary conditions (B.C.2) is always higher than for the first case (B.C.1).

2- For large Reynolds number, the power law index (n) of the Power law model has, for a given Reynolds and Prandtl numbers, a large effect on the heat transfer rate. The peak in average Nusselt number occurs between ($0.1 \leq n \leq 2$), depending upon Reynolds and Prandtl numbers. As the (Re) increases, the value of the power law index at which maximum average Nusselt number takes place shift towards lower values of (n) for all values of (Pr), while for small (Re), it does not have much effect on the heat transfer because in this situation, the convection is very weak and the dominant mode of energy transfer is conduction.

3- For Case(II), The maximum dimensionless temperature is always located at the middle of the bottom wall.

4- The study shows how to predict the effectiveness of a given duct in terms of energy transfer or to design an efficient one by suitably selecting the type of fluid or the shape of the duct or both.

References :

- [1] Yogosh, H., S., "Numerical Investigation of the Greetz Problem for Newtonian and Non-Newtonian Flows in Circular-Segment Ducts", M. Sc. Thesis, Univ. of Bombay (India), 2002.
- [2] Ibrahim, U., "Heat Transfer to a Power-law Fluid in Arbitrary Cross- Sectional Ducts" Kirikkal University, 2002.
- [3] J. M. Coulson, and J. S. Richardson, "Chemical Engineering", Bergamon, International Library, Vol. 3, 1983.
- [4] Myers, E., "Analytical Methods in Conduction Heat Transfer", Mc Graw – Hill Book Company, Inc., 1971.
- [5] L., S., Han, "Hydrodynamic Entrance Lengths for Incompressible Laminar Flow in Rectangular Ducts" Int. Journal of heat transfer, Vol. 27, pp 403-409, 2002.

- [6] Y., S., Muzychka, "Laminar Forced Convection Heat Transfer in the Combined Entry Region of Non- Circular Ducts" Int. Journal of heat transfer, Vol. 126, pp54-61,2004.
- [7] Najdat N., "Laminar Flow Separation in Constructed Channel", Ph.D. Thesis, Michigan State University, 1987.
- [8] Sparrow, E., M.,Haji-Sheikh, A., "Flow and Heat transfer in ducts of arbitrary shape with arbitrary thermal boundary conditions, Journal of Heat Transfer", Vol. 88 1966, pp. 351-358, vol. 91, pp. 588-589, 1969.
- [9] Frank, K., and Mark, S., "Principles of Heat Transfer", 5th Edition, PWS Publishing Company, 1997.

Table (1) Nusselt number comparison for the case of the square duct filled with Newtonian fluids and heated from the side for $Pr=0.71$.

Re	Nu_a	
	Muzychka.[9]	Present work
10^2	24.8267	24
10^3	24.99	24.5311
10^4	27.4679	25.471

Table (2) Nusselt number comparison for the case of the rectangular duct with Newtonian fluids and subjected to an ascending constant heat flux for ($Pr= 100$).

Re	Ar	Nu_a	
		Ibrahim, [2]	Present work
10^3	10^3	30.73982	30.556

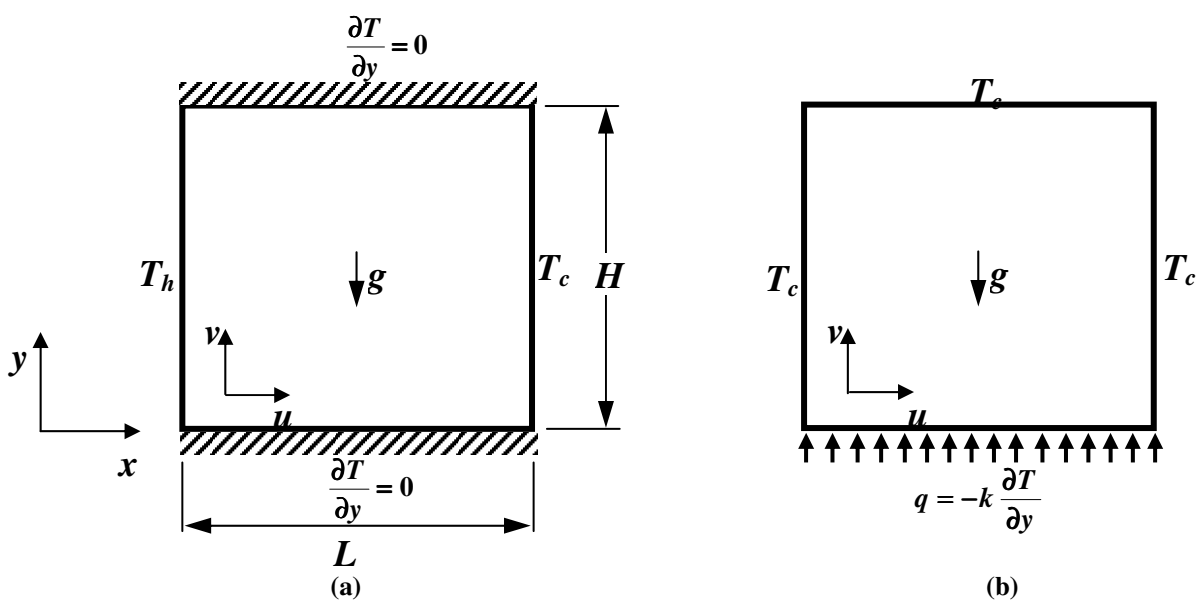


Fig.(1) Physical model and coordinate system. (a) case (I); (b) case (II)

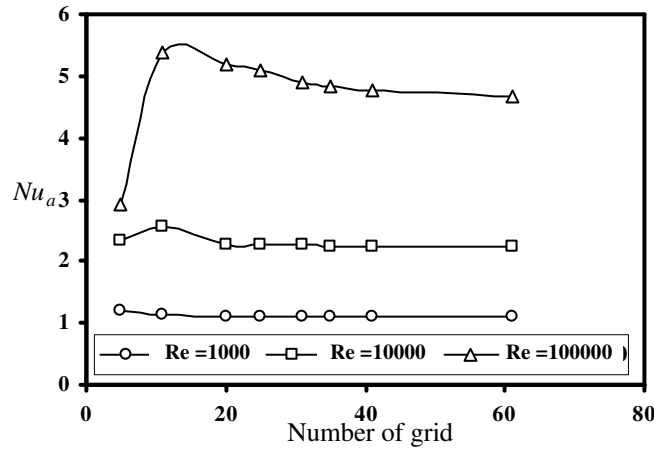


Fig.(2) Variation of Nusselt number with the number of grid points for different values of Reynolds number. Case (I) .

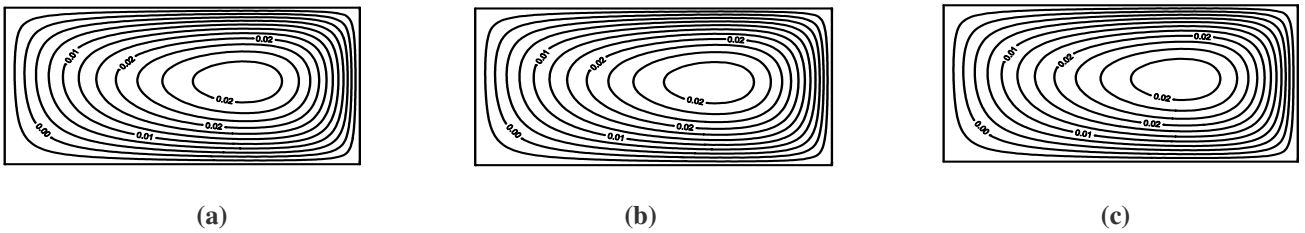


Fig.(3) Pattern of streamlines for $Re = 500$, $Ar = 0.5$ and $Pr=10$. (a) $n=0.1$, (b) $n=1$, (c) $n=2$. For Case (I)

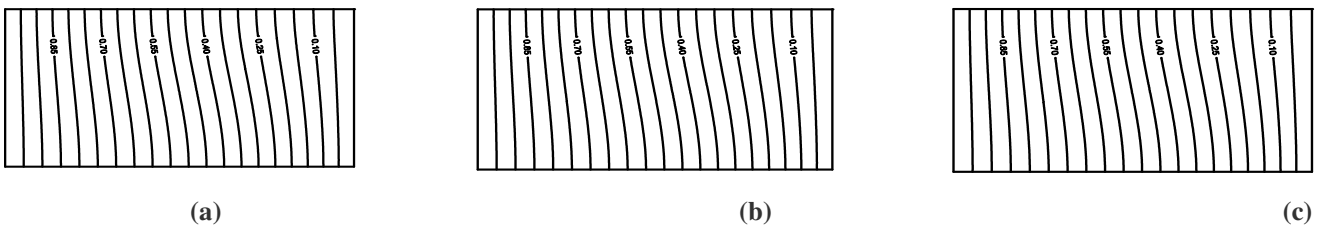


Fig.(4) Pattern of isotherms for $Re = 500$, $Ar = 0.5$ and $Pr=10$. (a) $n=0.1$, (b) $n=1$, (c) $n=2$. For Case (I)

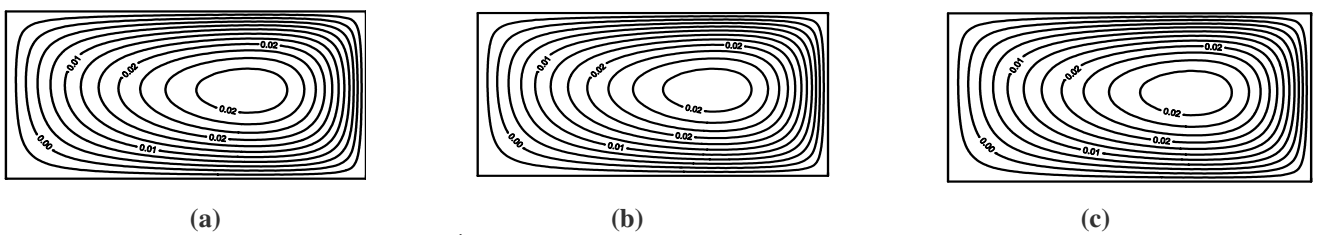


Fig.(5) Pattern of streamlines for $Re = 10^4$, $Ar = 0.5$ and $Pr=10$. (a) $n=0.1$, (b) $n=1$, (c) $n=2$. For Case (I)

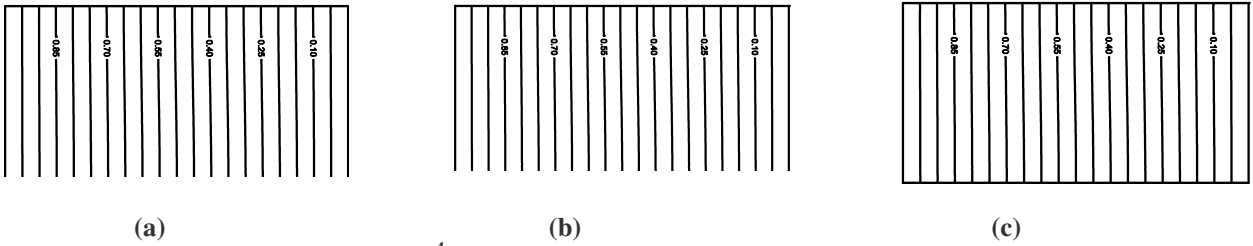


Fig.(6) Pattern of isotherms for $Re = 10^4$, $Ar = 0.5$ and $Pr=10$. (a) $n=0.1$. (b) $n=1$. (c) $n=2$. For Case (I)

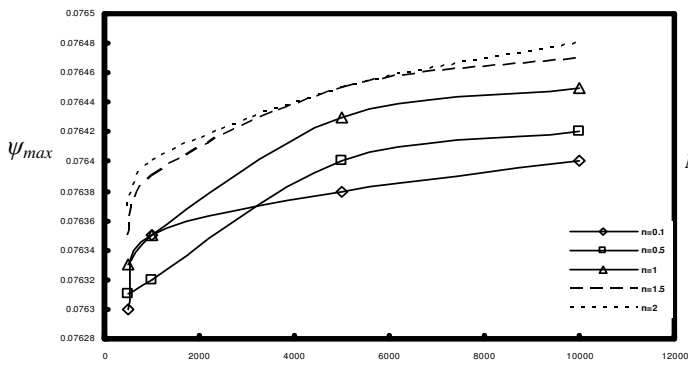


Fig.(7) Variation of $(\psi)_{max}$ with the Re for different values of n at $Ar=1.0$ and $Pr=10$. Case (I)

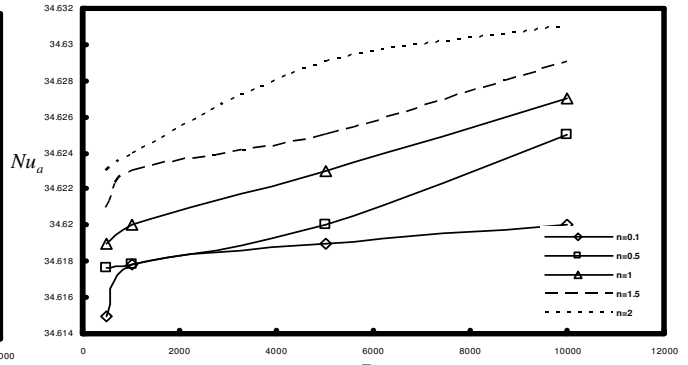


Fig.(8) Variation of Nu_a with the Re for different values of n at $Ar=1.0$ and $Pr=10$. Case (I)

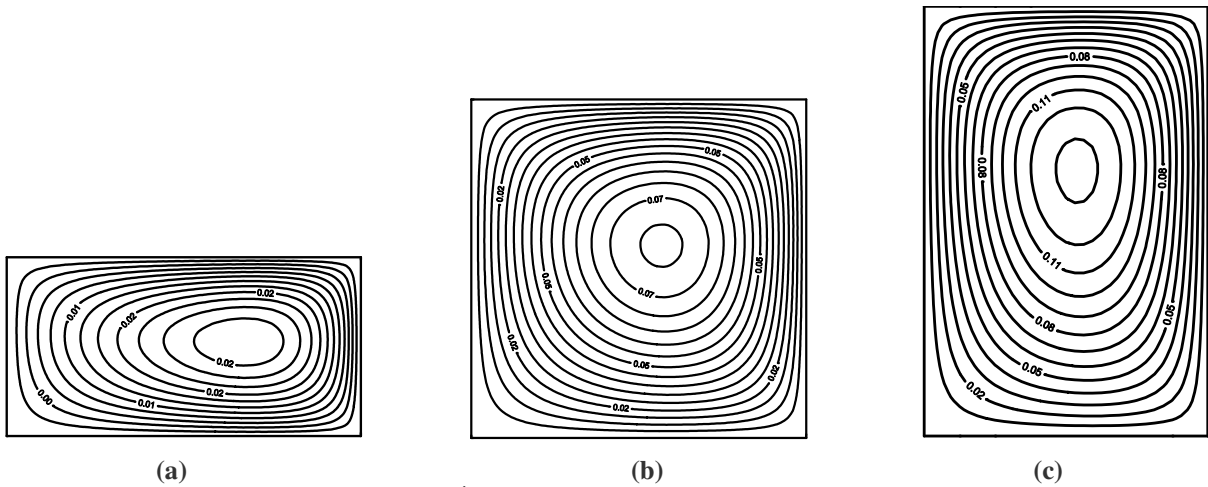


Fig.(9) Pattern of streamlines for $Re = 10^4$, $n = 2$ and $Pr=1$. (a) $Ar=0.5$, (b) $Ar=1$, (c) $Ar=1.5$. For Case (I)

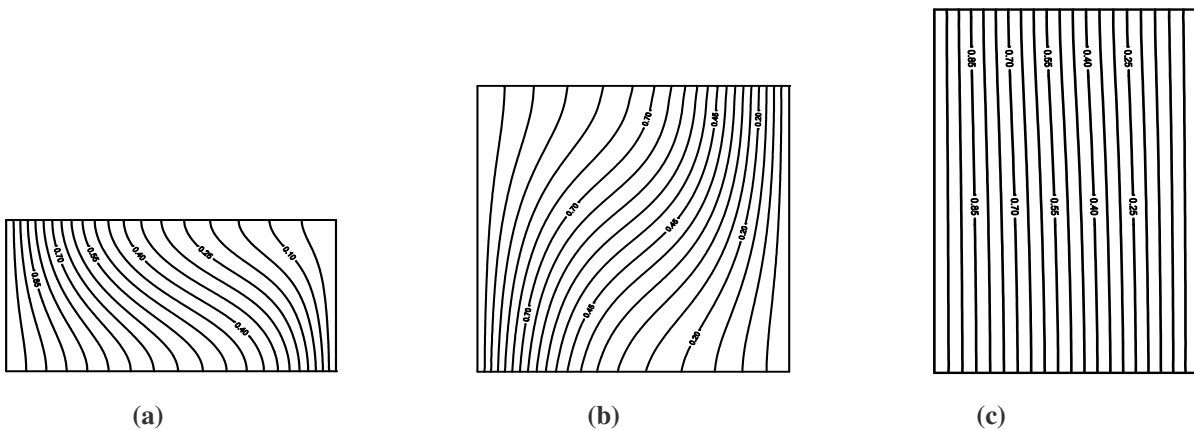


Fig.(10) Pattern of isotherms for $Re = 10^4$, $n = 2$ and $Pr=1$. (a) $Ar=0.5$, (b) $Ar=1$, (c) $Ar=1.5$. For Case (I)

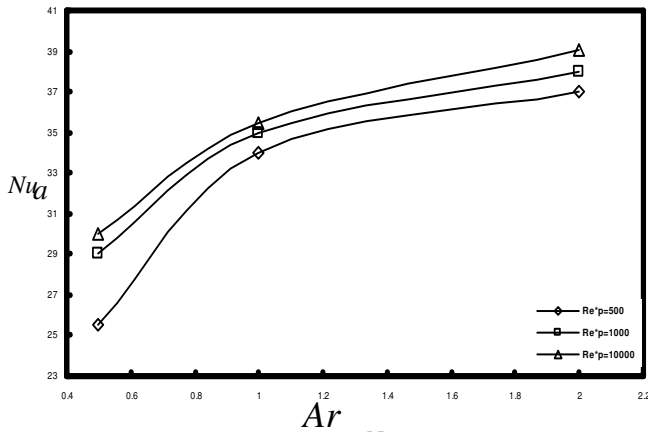


Fig.(11) Variation of Nu_a with the Ar for different values of Re at $n=1.5$ and $Pr=1$.

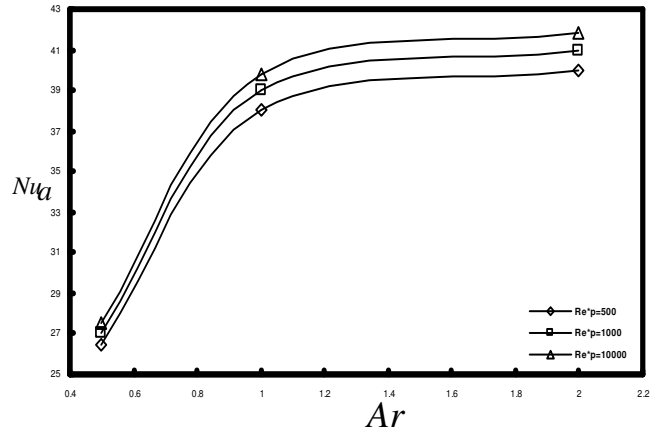
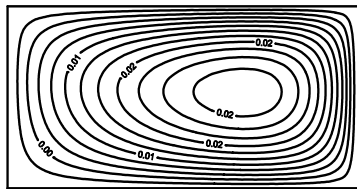
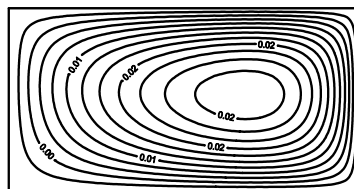


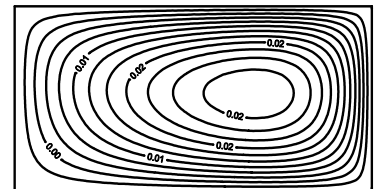
Fig.(12) Variation of Nu_a with the Ar for different values of Re at $n=1.5$ and $Pr=10$.



(a)



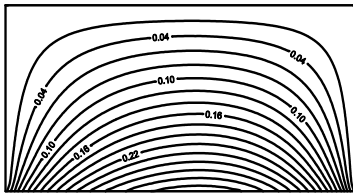
(b)



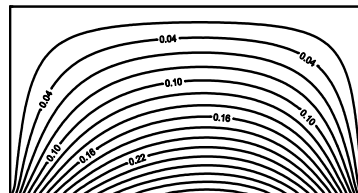
(c)

Fig.(13) Pattern of streamlines for $Re = 500$, $Ar = 0.5$ and $Pr=10$. (a) $n=0.1$, (b) $n=1$, (c) $n=2$.

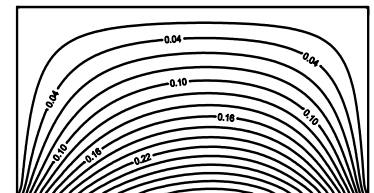
For Case (II)



(a)



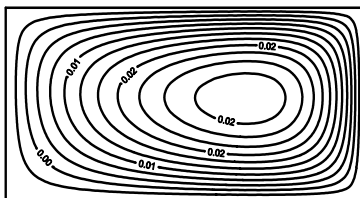
(b)



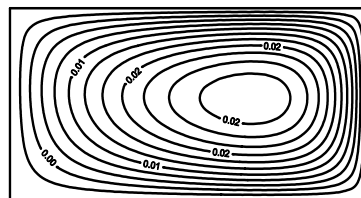
(c)

Fig.(14) Pattern Isotherms for $Re = 500$, $Ar = 0.5$ and $Pr=10$. (a) $n=0.1$, (b) $n=1$, (c) $n=2$.

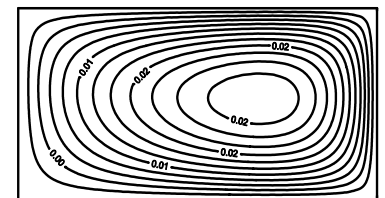
For Case (II)



(a)



(b)



(c)

Fig.(15) Pattern of streamlines for $Re = 10^4$, $Ar = 0.5$ and $Pr=10$. (a) $n=0.1$, (b) $n=1$, (c) $n=2$.

For Case (II)

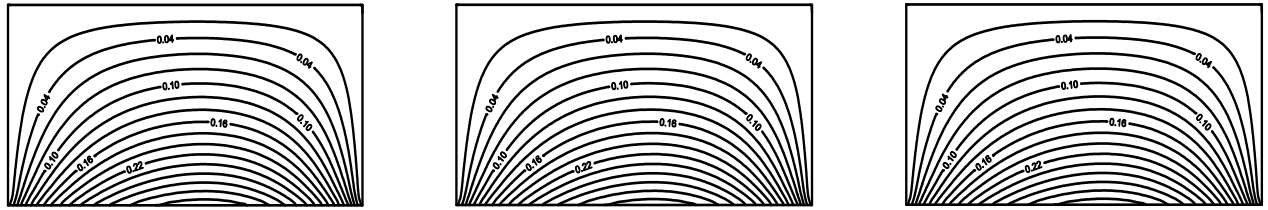


Fig.(16) Pattern Isotherms for $Re = 10^4$, $Ar = 0.5$ and $Pr=10$. (a) $n=0.1$, (b) $n=1$, (c) $n=2$. For Case (II)

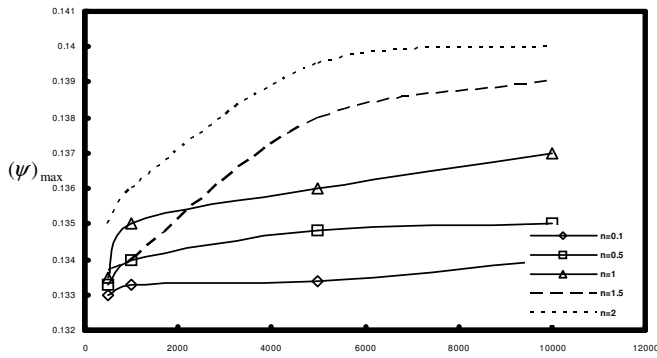


Fig.(17) Variation of $(\psi)_{max}$ with the Re for different values of n at $Ar=1.5$ and $Pr=1$. Case (II)

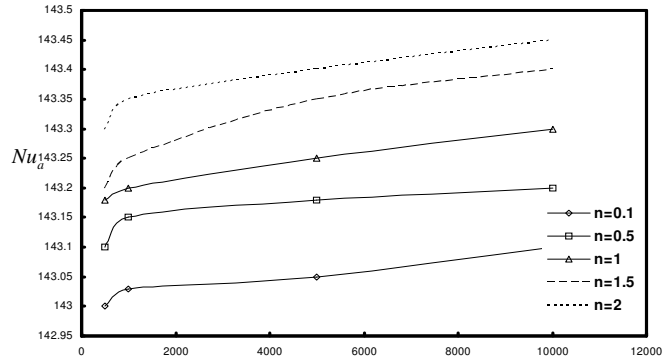


Fig.(18) Variation of Nu_a with the Ra_E for different values of n at $Ar=1.5$ and $Pr=1$. Case(II)

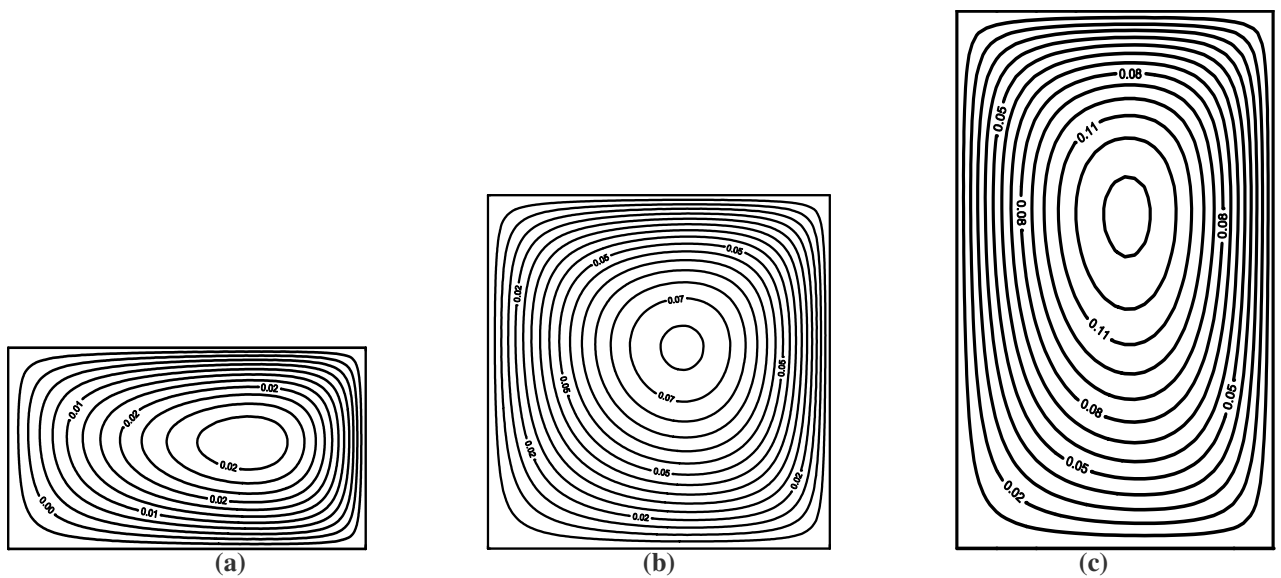


Fig.(19) Pattern of streamlines for $Re = 10^4$, $n = 2$ and $Pr=1$. (a) $Ar=0.5$, (b) $Ar=1$, (c) $Ar=1.5$. For Case (II)

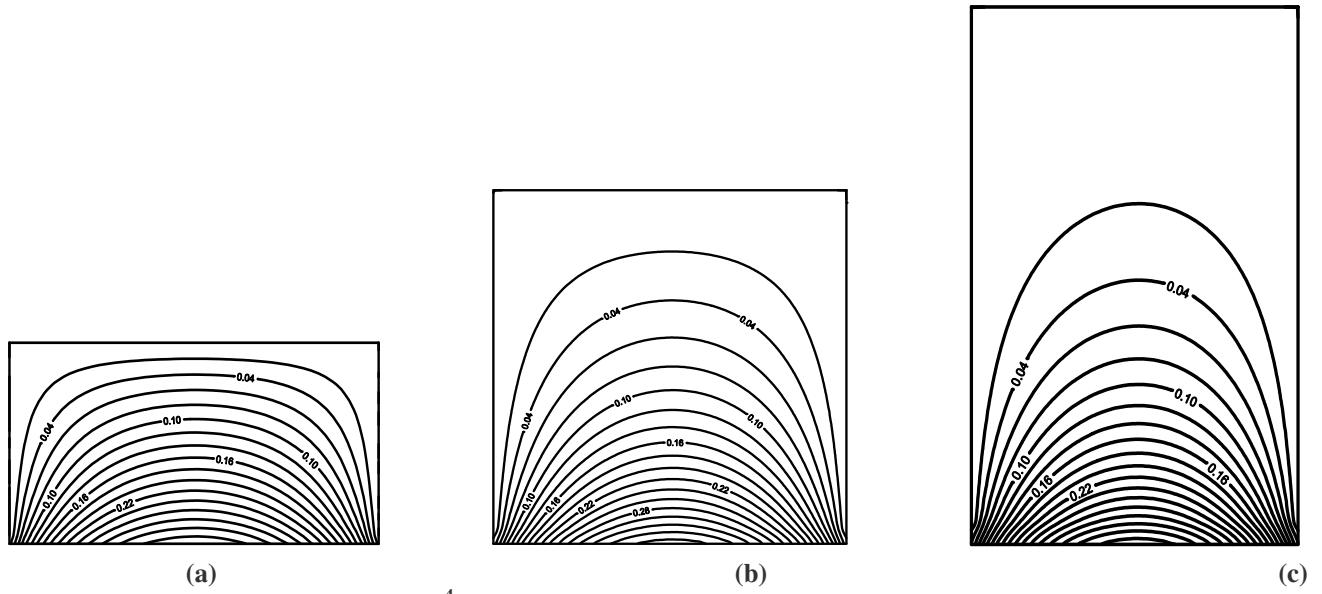


Fig.(20) Pattern of isotherms for $Re = 10^4$, $n = 2$ and $Pr = 1$. (a) $Ar = 0.5$, (b) $Ar = 1$, (c) $Ar = 1.5$.

For Case (II)

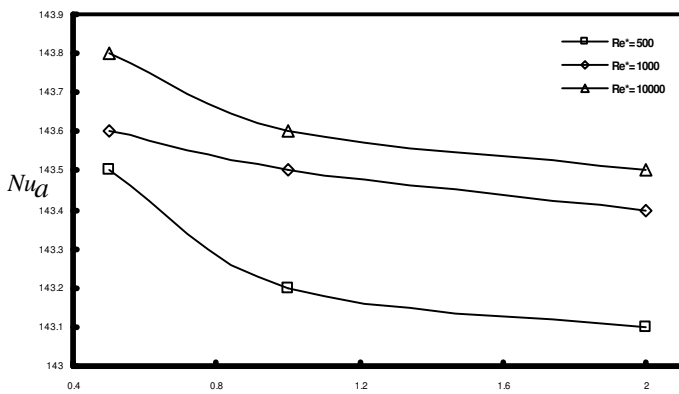


Fig.(21) Variation of Nu_a with the Ar for different values of Re at $n = 1.5$ and $Pr = 1$. Case (II)

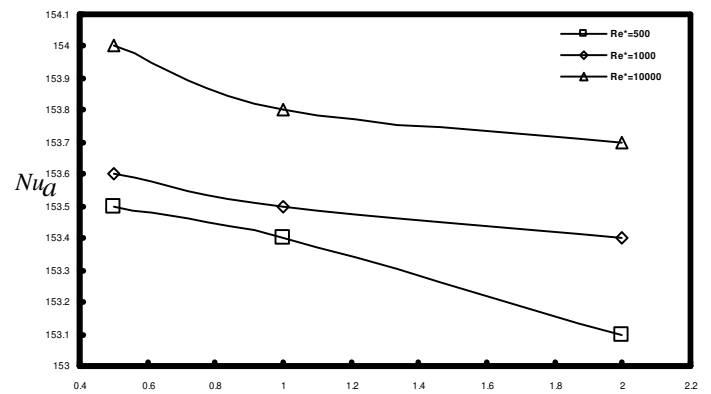


Fig.(22) Variation of Nu_a with the Ar for different values of Re at $n = 1.5$ and $Pr = 10$. Case (II)